

Elemental Mercury Adsorption Behaviors of Chemically Modified Activated Carbons

Byung-Joo Kim, Kyong-Min Bae,[†] Kay-Hyeok An, and Soo-Jin Park^{†,*}

Smart Composite Material Research Team, Carbon Valley R&D Division, Jeonju Institute of Machinery and Carbon Composites, 817 Duckjin-gu, Jeonju 561-844, Korea

[†]Department of Chemistry, Inha University, 253 Nam-gu, Incheon 402-751, Korea. *E-mail: sjpark@inha.ac.kr

Received November 17, 2010, Accepted February 28, 2011

In this work, the effects of different surface functional groups on the elemental mercury adsorption of porous carbons modified by chemical treatments were investigated. The surface properties of the treated carbons were observed by Boehm's titration and X-ray photoelectron spectroscopy (XPS). It was found that the textural properties, including specific surface area and pore structures, slightly decreased after the treatments, while the oxygen content of the ACs was predominantly enhanced. Elemental mercury adsorption behaviors of the acid-treated ACs were found to be four or three times better than those of non-treated ACs or base-treated ACs, respectively. This result indicates that the different compositions of surface functional groups can lead to the high elemental mercury adsorption capacity of the ACs. In case of the acid-treated ACs, the $R_{C=O}/R_{C-O}$ and R_{COOH}/R_{C-O} showed higher values than those of other samples, indicating that there is a considerable relationship between mercury adsorption and surface functional groups on the ACs.

Keywords : Elemental mercury, Chemically modified activated carbons, Surface functional groups

Introduction

Heavy metals are highly toxic at low concentrations and can accumulate in living organisms, causing several disorders and diseases. Mercury, which is a remarkably toxic and non-biodegradable metal, can be generated by several sources, resulting in critical contamination of atmospheric and aquatic systems.¹⁻⁴

On March 15, 2005, the US EPA issued the Clean Air Mercury Rule to permanently reduce Hg emissions from coal-fired power plants. The European Union considers mercury a priority and a hazardous pollutant and defines the maximum permissible concentration of total mercury as low as 1 µg/L for drinking water.⁵⁻⁸

Coal fired utility boilers are now identified as the major source of mercury. There is a strong global research imperative to find effective mercury control methods for coal combustion flue gases. Depending on the combustion conditions and flue gas chemistry, mercury compounds may be emitted as mercury oxide (Hg^{2+}) or elemental mercury (vapor) (Hg^0), due to their high volatility and vapor pressure.^{1,2,5-11}

The main techniques that have been used on heavy metal content reduction from industrial waste are chemical precipitation, ion exchange, membrane filtration, electrolytic methods, reverse osmosis, solvent extraction, and adsorption. Above all, adsorption, especially using activated carbons (ACs) as adsorbent, is currently the most widely used technology for mercury removal from incineration flue gases.¹²⁻¹⁸

Because of their extended surface area, high adsorption amount and rate, and specific surface reactivity, ACs have been widely used in waste water treatments to remove organic or inorganic pollutants. The adsorption capacity of ACs depends largely on many factors, such as raw materials,

activation process, the nature of the pore structure, and the surface functionality.^{19,20}

The existence of surface functional groups on carbons, such as carboxyl, phenol, lactone, and acid anhydrides has been postulated as constituting the source of surface acidity. Surface oxides on carbon surfaces can be formed by means of thermal treatment at high temperature, ozone treatment, and liquid treatment of chemical aqueous solutions.²¹ Normally, the surface treatments of carbons with acidic or basic chemical solution are performed to give functional groups, which improve adsorption capacity and selectivity on a certain adsorbate in gaseous or liquid phases.

Several of the studies²²⁻³⁰ referred to above have focused on methods of introducing a large number of surface functional groups. Still, the effects of the individual characteristics of these groups on elemental mercury adsorption have yet to be explicitly identified. Therefore, this paper is focused on the effects of surface functional groups on the elemental mercury adsorption capacity of ACs modified by chemical treatments.

Experimental Section

Sample Preparation. ACs supplied by Hanil GREEN TECH Co. of Korea (8 × 16 meshes) were used in this study. The ACs were obtained by chemical surface treatments in an aqueous solution of 35 wt % HCl (Acid-ACs) and 35 wt % NaOH (Base-ACs) for 24 h, thereby modifying the AC surfaces. Prior to use, the residue of the chemical solutions on the modified ACs was removed by Soxhlet extraction by boiling with acetone at 80 °C for 2 h. The treated ACs were washed several times with distilled water and dried in a vacuum oven at 85 °C for 24 h.

Surface pH and XPS Studies. The surface pH of the ACs was measured according to ASTM D3838, based on the boiling and sonic slurry method. In this procedure, about 1 g of ACs was added to 10 mL of boiled distilled water. The slurry was then heated until only sludge remained. After the sludge cooled to room temperature, its pH was measured with a glass pH electrode.

The acid and base values of the samples were determined by Boehm's titration method.³¹ In the case of the acid value, about 0.1 g of the sample was added to 100 mL of 0.1 N NaOH solutions and the mixture was shaken for 24 h. The solution was then filtered through a membrane filter and titrated with 0.1 N HCl solution. Likewise, the base value was determined by converse titration.

The XPS (ESCA210; VG Scientific Co.) spectra were collected using an MgK α X-ray source (1253.6 eV). The pressure inside the chamber was held below 5×10^{-8} torr during the analysis. The C_{1s} electron binding energy was referenced at 284.6 eV, and a curve-fitting procedure was carried out using a nonlinear least square curve-fitting program with a Gaussian-Lorentzian production function. For all elements, atomic concentrations were estimated based on comparisons of the integrated peak intensities normalized by the atomic sensitivity factors.

Textural Properties. N₂ adsorption isotherms were measured using a Belsorp Max (BEL Japan) at 77 K. The samples were degassed at 573 K for 12 h to obtain a residual pressure of less than 10^{-6} torr. The amount of N₂ adsorbed on the samples was used to calculate the specific surface area by means of the Brunauer-Emmett-Teller (BET) equation.³² The total pore volume was estimated to be the liquid volume of the N₂ at a relative pressure of approximately 0.995. The micropore volume was calculated using the *t*-plot method.³³

Mercury Vapor Adsorption. A 12.7 mm diameter reactor made of quartz was placed inside a temperature-controllable tubular furnace at a temperature of 70 °C. For every experiment, 1.0 g of samples were loaded and packed inside a quartz tube. A carrier gas was fed into the adsorption apparatus at a flow rate of 100 mL/min. Elemental mercury gas was generated from elemental mercury permeation tubes (Dynacalibrator[®] Model 150, VICI Metronics Inc., USA), and the concentration of the elemental mercury gas was maintained 800 $\mu\text{g}/\text{m}^3$ during the experimental process. Measurement of both the inlet and outlet concentration of the elemental mercury was done with a mercury analyzer (VM-3000, Mercury Instruments, Germany), and sulfur was used to capture the elemental mercury from the effluent gas.

Results and Discussion

Textural Properties. Chemical treatments, so-called acid-base treatments, are a well-known method to introduce surface functional groups containing oxygen onto carbon surfaces. Like other surface modification methods, these treatments can endow carbons with a number of polar functional groups but at the same time, cause the loss of some of their advantages, such as specific surface area or

Table 1. Textural Properties of Activated Carbons with Acid-Base Treatments

	S _{BET} ^a (m ² /g)	V _m ^b (cm ³ /g)	V _t ^c (cm ³ /g)	R _a ^d (nm)
Neat-ACs	1155	0.442	0.485	1.68
Acid-ACs	1138	0.436	0.471	1.66
Base-ACs	1062	0.421	0.434	1.63

^aSpecific surface area ($P/P_0 = 0.03-0.05$) = $V_{\text{ads}} \times 6.02 \times 10^{23} \times 1.62 \times 10^{-19} / 22400$. ^bMicropore volume (*t*-plot; thickness range = 0.6-2.0) = $[13.9900 / \{0.034 - \log(p/p_0)\}]^{0.5}$. ^cTotal pore volume = $V_{\text{ads}} \times (\text{molar volume of liquid N}_2 / \text{molar volume of gaseous N}_2)$. ^dAverage pore diameter (nm) = $4 \times V_{\text{tot}} / S_{\text{BET}}$

total pore volume.

Table 1 shows the textural properties of ACs before and after chemical treatments. It was observed that the specific surface area and pore volume decreased after each treatment. It is interesting to note that the average pore diameter decreased after each treatment from 1.68 nm to 1.63 nm. This indicates that the pore size distribution of the samples became narrower. The case of the Base-ACs sample shows the lowest value of average pore diameter in this work.

Figure 1 shows the N₂/77 K adsorption isotherms of the samples. It was found that each sample showed a typical Type I curve.³² It was found that the knee of the curves became sharper after the treatments, and that the Base-ACs showed the sharpest knee in this work. Normally, the sharpness of the isothermal curve leads to a narrow pore size distribution. In Table 1, we can see that the average pore size became narrower after the treatments.

It is well-accepted that surface oxidation treatments, including acid-base treatments can introduce surface functional groups on the carbon surfaces. Newly-formed functional groups can be placed on the flat surface, near the pore entrance, or on the pore walls. In the case of the pore walls, the size of the pore diameters can be reduced, indicating that some narrow mesopores can be turned into micropores, resulting in a decrease of average pore diameter.

In Figure 1, it can be observed that the increase tendency

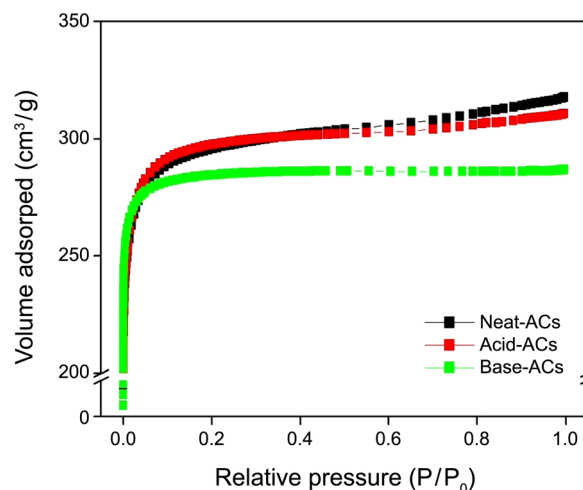


Figure 1. N₂/77 K adsorption isotherms of activated carbons before and after chemical treatments.

Table 2. pH and Acid-Base Values of Activated Carbons with Acid-Base Treatments

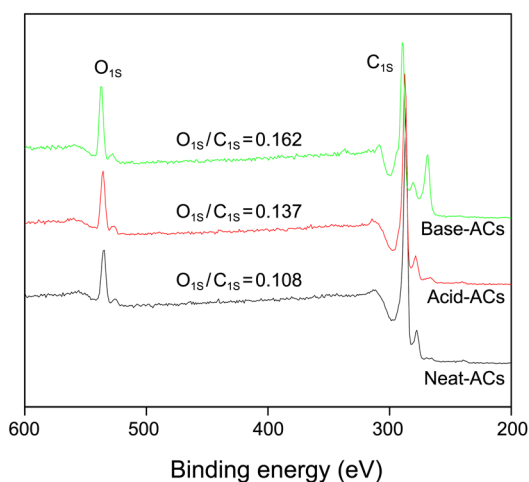
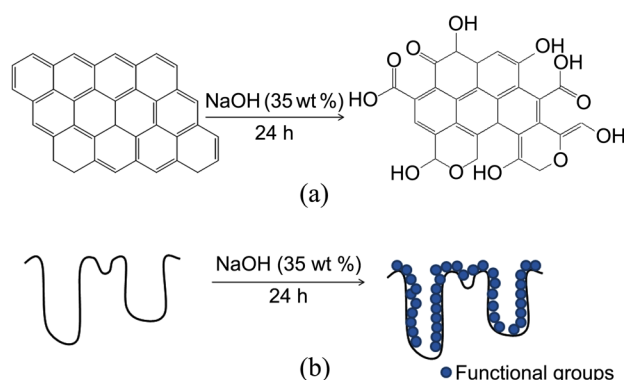
	pH	Acid value (meq/g)	Base value (meq/g)
Neat-ACs	7.4	110	130
Acid-ACs	6.2	175	85
Base-ACs	8.1	65	220

of Acid-ACs declined in the high region of relative pressure, compared with that of Neat-ACs. This result supports that the idea that some meso- or macropores were blocked or turned into sub-pores after the treatments. This phenomenon is more obviously observed in the Base-ACs.

Surface Properties. Table 2 shows the pH and acid-base values of the samples before and after chemical treatments. It was found that the surface pH of Acid-ACs and Base-ACs are 6.2 and 8.1, respectively. As expected, the acid value of the Acid-ACs and the base value of the Base-ACs are predominantly enhanced after the treatments. These results indicate that the sample surfaces are successfully improved, which was the experimental purpose.

To confirm the changes of the surface functional groups on the carbon surfaces, XPS studies were used, with results shown in Figure 2. It shows the XPS survey spectra of the ACs before and after chemical treatments. It was observed that C_{1s} peaks decreased and O_{1s} peaks increased after each treatment. These results indicate that C=C, C-C, or C-H groups on the AC surfaces can be broken and can form new functional groups containing oxygen, such as C-O, C=O, or COOH. It was also found that the O_{1s}/C_{1s} ratio of the Base-ACs showed its best value (0.162), meaning that the surface etching could be violent in the condition of 35 wt % NaOH for 24 h.

Figure 3(a) shows a schematic of the surface etching behaviors after surface treatments. It shows that outer graphitic structure is etched and newly forms oxygen functional groups. This reaction can cause high oxygen content on the carbon surface. Meanwhile acid treatments can convert some functional groups to the further oxidized func-

**Figure 2.** XPS survey spectra of activated carbons before and after chemical treatments.**Figure 3.** Surface etching reaction (a) and a schematic of the pore narrowing behavior (b) after surface treatments.

tional groups, such as the carbonyl or carboxylic acid group. Figure 3(b) is a schematic of pore narrowing effects. The base treatments can cause many functional groups on the carbon surface. These functional groups may form pore walls or entrances, resulting in pore narrowing or blocking in the excessively oxidized area. The behaviors can lead the sharp knee in the adsorption isotherm curves.

To observe the formation behavior of surface functional groups on the ACs, high resolution C_{1s} and O_{1s} peaks were studied, with results shown in Figures 4 and 5. It was seen that the AC surfaces were composed of various surface functional groups, including phenolic hydroxyl groups (C-OH or -C-O-), carbonyl groups (C=O), or carboxylic acid groups (-COOH). It was also observed that the specific ratio of the C=O or COOH groups increased after the treatments (The absolute content of the oxygen functional groups of the Acid-ACs and the Base-ACs is much higher than that of the Neat-ACs.). The total ratios of the oxygen functional groups in the C_{1s} peaks were 42% (Neat-ACs), 43.7% (Acid-ACs), and 48.7% (Base-ACs).

It is interesting to note that the ratio of C=O and COOH groups at the treated-ACs shows a different composition. In the case of the Acid-ACs, the ratios of C=O and COOH groups were predominantly enhanced while the C-O ratio decreased from 26.5% to 23.1%. Meanwhile, in the Base-ACs, the C-O ratio increased significantly to 28.0%, while ratios of C=O and COOH groups were 13.2% and 7.5%.

These behaviors lead to the idea that each sample was prepared under different reaction circumstances. The Acid-ACs showed a decrease of the C-O ratio and an increase of the C=O and COOH ratios. This indicates that some of the C-O groups turned into C=O and COOH due to further oxidation conditions. Meanwhile, in the Base-ACs, the C-O, C=O, and COOH ratios increased, meaning that C-C or C-H breaking mainly occurred and formed new oxygen functional groups.

Figure 5 shows high resolution and shows O_{1s} peaks of ACs before and after chemical treatments. These figures show mainly C-O, C=O, and O-C=O peaks. It was found that the specific ratios of C-O, C=O, O-C=O in the Acid-ACs showed very similar patterns with that of the C_{1s} peaks. The C-O ratio decreased, and the C=O and O-C=O were

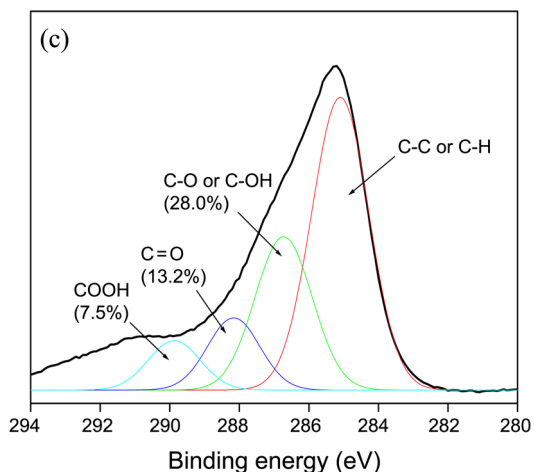
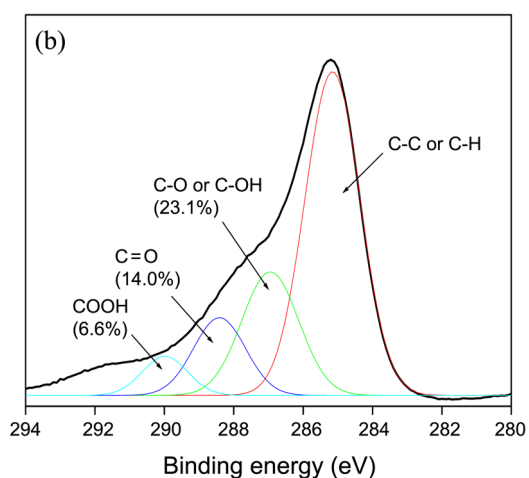
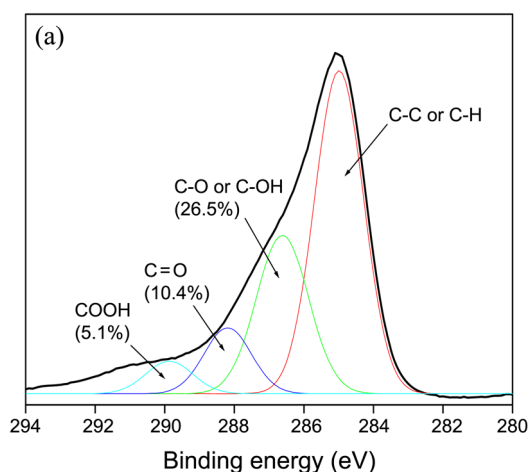


Figure 4. High resolution of C_{1s} peaks of activated carbons before and after chemical treatments; (a) Neat-ACs, (b) Acid-ACs, (c) Base-ACs.

significantly enhanced. Meanwhile, the C-O ratio in the Base-ACs was dramatically improved. These behaviors can be seen as a good proof to support the idea that a further oxidation reaction occurred in the Acid-ACs and that the surface etching reaction mainly occurred in the Base-ACs, as mentioned above. Table 3 lists the functional group ratios between C-O and other samples, such as $R_{C=O}/R_{C-O}$ and

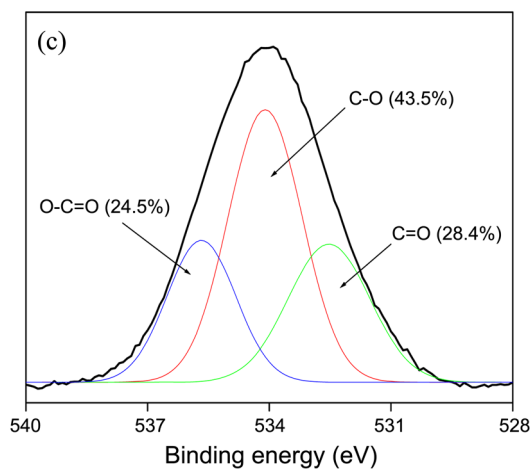
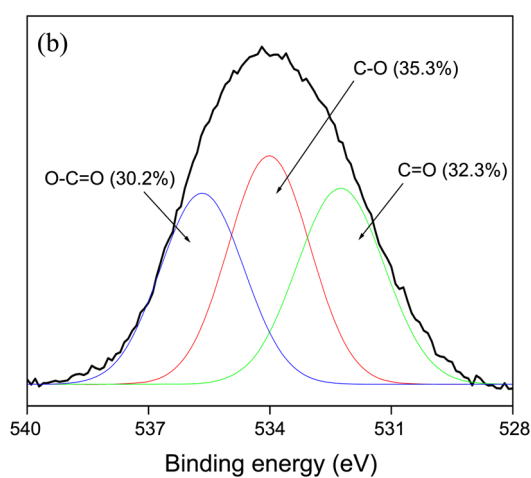
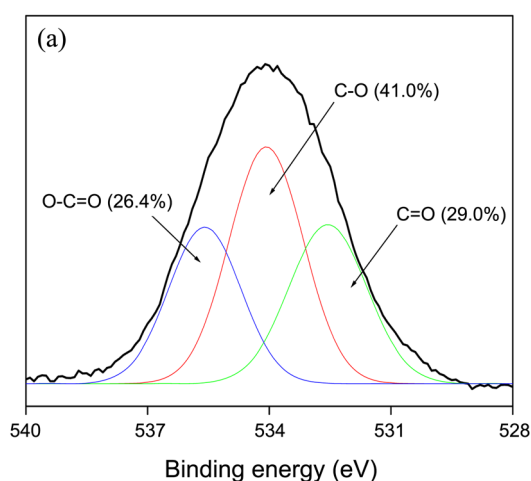


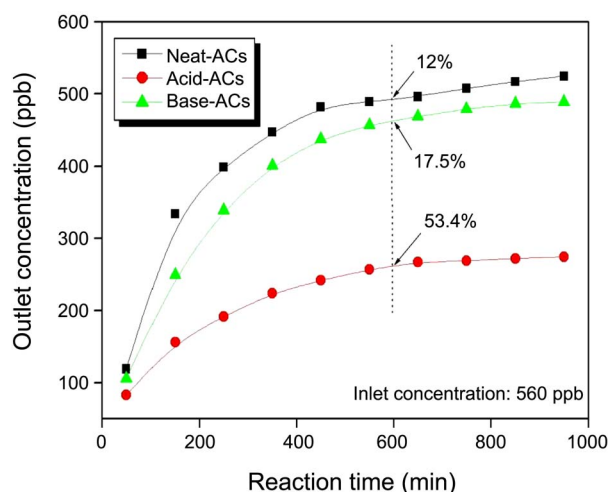
Figure 5. High resolution of O_{1s} peaks of activated carbons before and after chemical treatments; (a) Neat-ACs, (b) Acid-ACs, (c) Base-ACs.

R_{COOH}/R_{C-O} . This table clearly shows that the excessive oxidation reactions occurred with Acid-ACs sample.

Elemental Mercury Adsorption. Figure 6 shows the elemental mercury adsorption of the as-received sample and of the ACs before and after acid-base treatments. All tests were conducted at 70 °C for 1 h in the elemental mercury adsorption apparatus. The Neat-ACs showed only low

Table 3. Specific Ratio of $R_{C=O}/R_{C-O}$ and R_{COOH}/R_{C-O} in High Resolution C_{1s} and O_{1s} Peaks

	C_{1s}		O_{1s}	
	$R_{C=O}/R_{C-O}$	R_{COOH}/R_{C-O}	$R_{C=O}/R_{C-O}$	R_{COOH}/R_{C-O}
Neat-ACs	0.39	0.19	0.71	0.64
Acid-ACs	0.60	0.29	0.92	0.86
Base-ACs	0.47	0.27	0.65	0.56

**Figure 6.** Elemental mercury adsorption behaviors of activated carbons before and after chemical treatments.

elemental mercury adsorption of 12% (67.2 ppb) at 600 min. The Acid-ACs showed an elemental mercury adsorption result of 53.4% (299 ppb) at 600 min, thus showing higher elemental mercury adsorption than that of the other samples. The Base-ACs didn't show better mercury adsorption capacity than that of Acid-ACs.

Normally, gas-phase adsorption of ACs is ruled by two factors, specific surface area including porous structures, and surface activity, indicating catalyst loaded or surface functional groups.

In this work, the specific surface area of the Base-ACs is not lower than that of the Acid-ACs. However, the mercury removal efficiency of the Acid-ACs is three times higher than that of the Base-ACs. This result indicates that the specific surface area or the pore structures are not key factors to control mercury adsorption capacity in this system. Then, the main difference of between the two samples is the specific composition of the surface functional groups. As can be seen in Figures 3 and 4, the Acid-ACs have a higher portion of excessively oxidized functional groups, C=O and COOH, than that of the Base-ACs. In the data shown in Table 2, we can see that the acid value of the Acid-ACs was absolutely higher than that of the Base-ACs.

From these results, it can be concluded that elemental mercury molecules have good chemical affinity with acidic functional groups, the so-called electron acceptors. Normally, metal species have a strong polar nature. Molecules that have acidic natures normally demonstrate good chemical

affinity with adsorbent having basic natures, due to the acid-base interaction.³⁴ In our previous work, we found that hydrogen molecules easily adsorbed on the surface of the Ni-coated carbon materials. The total content of hydrogen adsorbed at room temperature was enhanced with the metal content on the carbon. From this work, we proposed the partially induced-dipole behavior of hydrogen molecules, and found they acted like base natures (electron-donors) on the Ni-coated carbon surfaces (electron-acceptor).^{35,36}

In present work, we found that elemental mercury can be adsorbed on ACs having acidic surface functional groups (electron acceptor surfaces). So, from the results, elemental mercury adsorption behavior indicates that elemental mercury molecules (vapor) can have base natures (electron donor) even though we can't fully check the chemical reaction between mercury and carbon molecules themselves from the ACs.

Conclusions

In this work, the effects of different surface functional groups on the elemental mercury adsorption of porous carbons modified by chemical treatments were investigated. This result indicates that the different composition of surface functional groups can lead the high elemental mercury adsorption capacity of the ACs. In case of the acid-treated ACs, the $R_{C=O}/R_{C-O}$ and R_{COOH}/R_{C-O} showed higher values than other samples, indicating that elemental mercury molecules can have electron donor nature in this work

Acknowledgments. This subject is supported by Korea Ministry of Environment as "The Eco-technopia 21 Project".

References

- Darbha, G. K.; Singh, A. K.; Rai, U. S.; Yu, E.; Yu, H.; Yu, H.; Ray, P. C. *J. Am. Chem. Soc.* **2008**, *130*, 8038.
- Issaro, N.; Abi-Ghanem, C.; Bermond, A. *Anal. Chim. Acta* **2009**, *631*, 1.
- Pavlish, J. H.; Hamre, L. L.; Zhuang, Y. *Fuel* **2010**, *89*, 838.
- Ji, H.; Kim, J.; Yoo, J. W.; Lee, H. S.; Park, K. M.; Kang, Y. *Bull. Korean Chem. Soc.* **2010**, *31*, 1371.
- ShamsiJazeyi, H.; Kaghazchi, T. *J. Ind. Eng. Chem.* **2010**, *16*, 852.
- Galbreath, K. C.; Zygarlicke, C. J. *Fuel Process. Technol.* **2000**, *65*, 289.
- Xin, G.; Zhao, P.; Zheng, C. *Proc. Combustion Inst.* **2009**, *32*, 2693.
- Jeon, S. H.; Eom, Y.; Lee, T. G. *Chemosphere* **2008**, *71*, 969.
- Kwon, S. K.; Kim, H. N.; Rho, J. H.; Swamy, K. M. K.; Shanthakumar, S. M.; Yoon, J. *Bull. Korean Chem. Soc.* **2009**, *30*, 719.
- Skodras, G.; Diamantopoulou, I.; Pantoleonos, G.; Sakellaropoulos, G. P. *J. Hazard. Mater.* **2008**, *158*, 1.
- Ghodbane, I.; Hamdaoui, O. *J. Hazard. Mater.* **2008**, *160*, 301.
- Portzer, J. W.; Albritton, J. R.; Allen, C. C.; Gupta, R. P. *Fuel Process Technol.* **2004**, *85*, 621.
- Pitoniak, E.; Wu, C. Y.; Mazzyck, D. W.; Powers, K. W.; Sigmund, W. *Environ. Sci. Technol.* **2005**, *39*, 1269.
- Vidic, R. D.; Siler, D. P. *Carbon* **2001**, *39*, 5763.
- Manoochhri, M.; Rattan, V. K.; Khorsand, A.; Panahi, A. *Carbon*

- Lett.* **2010**, *11*, 169.
16. Karatza, D.; Lancai, A.; Musmarra, D.; Zucchini, C. *Exp. Therm. Fluid Sci.* **2000**, *21*, 150.
17. Ghorishi, S. B.; Robert, M. K.; Shannon, D. S.; Brian, K. G.; Wojciech, S. J. *Environ. Sci. Technol.* **2002**, *36*, 4454.
18. Fathy, N. A.; El-Sherif, Y. *Carbon Lett.* **2011**, *12*, 1.
19. Bansal, R. C.; Donnet, J. B.; Stoeckli, F. *Active Carbon*; Marcel Dekker: New York, 1988.
20. Suffet, Y. H.; McGuire, M. J. *Activated Carbon Adsorption*; Ann Arbor Science: Michigan, 1981.
21. Choi, W. K.; Kim, B. J.; Chi, S. H.; Park, S. J. *Carbon Lett.* **2009**, *10*, 239.
22. Park, S. J.; Kim, B. J. *J. Colloid Interface Sci.* **2005**, *291*, 597.
23. Calvert, S., Englund, H. M. *Handbook of Air Pollution Technology*; John Wiley & Sons: New York, 1984.
24. Kim, B. J.; Park, S. J. *J. Colloid Interface Sci.* **2010**, *342*, 575.
25. Cho, K. S.; Kim, B. J.; Kim, S.; Kim, S. H.; Park, S. J. *Bull. Korean Chem. Soc.* **2010**, *31*, 100.
26. Lee, S. J.; Seo, Y. C.; Jurng, J.; Lee, T. G. *Atmos. Environ.* **2004**, *38*, 4887.
27. Li, Y. H.; Lee, C. W.; Gullett, B. K. *Fuel* **2003**, *82*, 451.
28. Skodras, G.; Diamantopoulou, I.; Sakellariopoulos, G. P. *Desalination* **2007**, *210*, 281.
29. Zhu, J.; Deng, B.; Yang, J.; Gang, D. *Carbon* **2009**, *47*, 2014.
30. Hu, C.; Zhou, J.; Luo Z.; He, S.; Wang, G.; Cen, K. *J. Environ. Sci.* **2006**, *18*, 1161.
31. Boehm, H. P. *Adv. Catal.* **1966**, *16*, 179.
32. Brunauer, S.; Emmett, P. H.; Teller, E. *J. Am. Chem. Soc.* **1938**, *60*, 309.
33. Lippens, B. C.; de Boer, J. H. *J. Catal.* **1965**, *4*, 319.
34. Park, S. J. *Interfacial Forces and Fields: Theory and Applications*; Marcel Dekker: New York, 1999.
35. Kim, B. J.; Lee, Y. S.; Park, S. J. *Int. J. Hydrogen Energy* **2008**, *33*, 4112.
36. Kim, B. J.; Park, S. J. *Int. J. Hydrogen Energy* in press.
-